LUT UNIVERSITY
LUT School of Energy Systems
LUT Mechanical Engineering

Oscar Chia Moradi

IMPROVEMENT OF THE MEASURING ACCURACY OF MEASURING SCANNER BY ISOLATION OF CIRCUMSTANTIAL FACTORS

Examiner(s): Professor Heikki Handroos
D.Sc. Hamid Roozbahani

ABSTRACT

LUT University
LUT School of Energy Systems
LUT Mechanical Engineering

Oscar Moradi

Improvement of the Measuring Accuracy of Measuring Scanner by Isolation of Circumstantial factors

Master's thesis

2019

49 pages, 37 figures, 8 table

Examiners: Professor Heikki Handroos
D.Sc. Hamid Roozbahani

Keywords: Vibration, temperature fluctuation, measuring accuracy.

Measuring accuracy of a measuring scanner is important, there are several factors that affect the measuring accuracy, such as vibration, temperature fluctuation, material of the scanner and electrical insulation.
In this thesis, vibration and the temperature fluctuation of the machine are studied, and corresponding components are selected to eliminate the effects. Vibration can be generated from the ground and from direct connect as well, the vibration is measured by using vibrometer. And the collected data is charted by using excel sheet, then suitable vibration pads can be selected based on the analysis of the collected data. As for the temperature fluctuation, the structure is made by aluminum, there will be contraction and expansion of the structure changes when the temperature fluctuates in Finland. Theory calculation by hand calculation and FE analysis are carried, then suitable climate control system is selected. Furthermore, suitable insulation is selected.

ACKNOWLEDGEMENTS

I would like to thank the all Finnos coworker for their participation in the data gathering that supported my work. I am also grateful to The CEO of Finnos Jere Heikkinen for support in overcoming numerous obstacles I have been facing through my research and timetable.

I would like to thank my supervisor Professor Heikki Handroos for his support and helping me with his tolerant as I was slow on the progress on the thesis due to working entire time.

Oscar Chia Moradi
Lappeenranta 1.9.2019

TABLE OF CONTENTS

LIST OF SYMBOLS AND ABBREVIATIONS

q	Heat transfer [W]
dT	Temperature difference [°C]
U	The overall heat transfer coefficient [W/(m^{2}K)]
A	Wall area [m^2]
$h_{c,i,o}$	Inside or outside wall individual fluid convection heat transfer coefficient [W/(m^{2}K)]
s	Thickness of layer [m]
k	Thermal conductivity of material [W/(mK)]

1 INTRODUCTION

Nowadays, sawmill industry in Finland is mature due to the abundant resource come along with the reasonable usage. The role of sawmill industry and the related wood products have received increased attention across a number of disciplines in the forest resources, among which the sustainability of the forestry is one of the most important issue that attracts human beings in recent years. There are quite many views that sawmill industry should concern about. In our case, to design a machine that can help sort and cut the logs is the mission.

The motivation of the researches comes from the situation that there is lack of existed integrated product. There are several commercial scanners in the market, but they have problems in vibration absorption, thermal expansion and shrinking, as well as other problems that will affect the measuring accuracy, which is one of the most crucial function of the scanners and play a key role in all kinds of the measurement tool. In the real situation, there are many factors affect the measuring accuracy and they are not possible to eliminate. For example, in the machine manufacturing phase, there are manufacturing deviation, in the machine assemble phase, there are assemble error depends on the assemble methods, such as welding, and this is the reason that in some case, after welding, there will be measurement and inspection following, then the new design will be made after this to compensate the error. Moreover, there are also environment factors, such as weather, especially in Finland, the weather differs from -30℃ to 30℃, and the humidity, which will affect the structure shell and decide if the coating is needed. Another problem occurs if the product is shipped to other country around the world, the environment factors will be totally different. Therefore, the importance of the controlling the factors that affect measuring accuracy is crucial, which make the vibration and temperature insulation study in this thesis.

The outline of this thesis can be divided into four parts. The first part is the introduction, which tells the background of the topic. Then in the second part, the methods related to the vibration and temperature measurement are introduced separately in literature review and practical work. The third part tells the experiment results of the measurement and the corresponding solutions are carried out. And in the end, the analysis based on chosen devices are mentioned as well as future of the topic.

In this chapter, the sections will be arranged as follow. In the first part, brief introduction about Finnos and the product will be introduced, which tells what the product is, why should sawmill industry needs the technology and the machine and how the machine works. In the second sections, some existed products are introduced to help the readers to understand this kind of machines better. The last part introduces the main topic of this thesis, which are vibration and temperature, those are the circumstantial factors that affect the measuring accuracy. There are also some other parameters affect the measuring result, such as internal components accuracy of the machine, but here focus would be on two parameters, vibration and temperature. All in all, focus on the component's selection and some theory behind them are studied. And research question here is that will the components selected can improve the equipment stability. There are other researches related in mathematic ways for example from Jere (Siltanen et al., 2003, Mendoza et al., 2019).

1.1 Brief introduction about the product

There are many solutions offered from Finnos, they can produce promising and accurate data on log quality starting from sorting. Then the data can be used in many purposes, such as determining the value of a log to see if this log satisfy the customer needs. Finnos systems offer significant improvements in terms of raw materials consumption, quality yield and productivity in sawmill, pulp, energy and plywood industries. (Finnos Oy, 2019)

It cost about 4 to 5 euros per cubic meter of raw material in sawmill industry nowadays. However, by optimizing wood sorting, the benefit on cost is that about 20% cost will be saved in measuring barkless log top diameter accurately. (Finnos Oy, 2019)

There are several solutions, and the advantages come along are less waste, more results for the sawmill industry. There are several ways that can dramatically improve the productivity in cutting edge log measuring system. Finnos incorporates advanced laser and X-ray technology is one option. The system is user friendly and the operator just need some basic training and then they are able to use the system to control sorting accurately, end up producing consistent quality and efficient use of raw material. The designed machine is a cubic steel structure, sized around 3000 mm x 2400 mm x 2500mm. It can measure on going logs through the conveyor with speed of 4 meters per second. And the detail jobs include

measuring diameter, shape geometry, thickness of the bark, defects, knots, hard wood parts, and age.

The mechanical components involved in this machine includes laser generator, laser cameras, RGP cameras, X-ray generators and X-ray detectors, the total amount of the cameras is 17 and there are also two direction X-ray. The mass of the cubic structure is around 4800 kg. (Finnos Oy, 2019)

- Fusion log scanner

This is one advanced comprehensive solution shown in **Figure 1**. The fusion log scanner is set in a shipping container, the system combines advanced laser and X-ray measurement technologies. With the utlilization of the software, the data can be used depends on purpose and integrated with production management and other information systems. In the end, this solution will maximize benefits while minimize the waste at the same time. Finnos Oy, 2019)

Figure 1. Fusion log scanner. (Finnos Oy, 2019)

- Lite log scanner

This is modular light system shown in **Figure 2**. The Lite system is designed for smaller applications with cost-efficient solution in productivity. The key benefit of the solution is significant raw material savings gained through accurate top diameter measurements. The system can be modified with modules to meet increased sorting needs. (Finnos Oy, 2019)

Figure 2. Lite log scanner. (Finnos Oy, 2019)

Log roller optimizer

Figure 3.

By checking the position and orientation of logs, the system can optimize the results with modular X-ray unit, which allowing log orientation based on branch locations and log internal characteristics. (Finnos Oy, 2019)

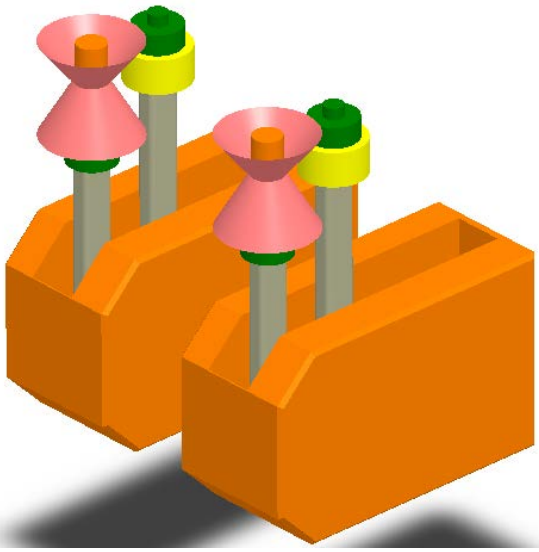

Figure 3. Log roller optimizer. (Finnos Oy, 2019)

1.2 Existed concept or products

In this section, existed concept and products are introduced, they are quite familiar with Finnos products, there are some differences on the function, but the ideas of these two products are helping to give reader overall picture. Here are the products in the field of wood log scanning. And two of them will be introduced.

1.2.1 Goldeneye 500

Here is the first product and this product is called Goldeneye 500 from MICROTEC shown in **Figure 4**, it is multi sensor quality scanner for log, it can grading, chopping and sorting for joinery and wood component. (Microtec.eu, 2019)

Figure 4. Goldeneye 500. (Microtec.eu, 2019)

In this product, X-ray technology sensors, state-of-the-art cameras and other components are integrated into this product. It can help the customers to recognize log defects automatically in a reliable and accurate way. The customer can customize the specific grading, chopping and sorting rules and the machine can justify based on these rules. An illustration of the scanning log can be seen in **Figure 5**. (Microtec.eu, 2019)

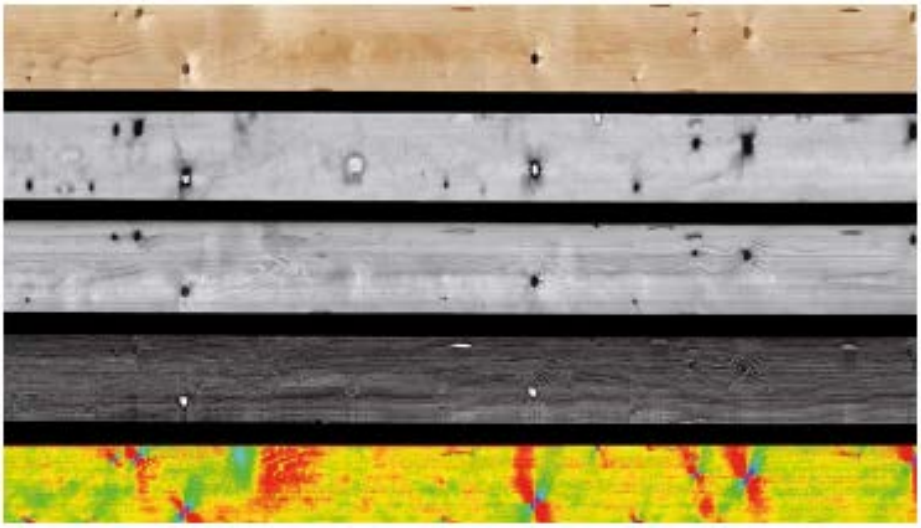

Figure 5. Log scanning result. (Microtec.eu, 2019)

Some of the product features are:

- Multi-sensor cameras and sensors
- X-ray technology to identify wood defects that are not visible on the surface and to determine the internal structure of the log
- Color scanning with full HD resolution
- Laser 3D triangulation
- Laser scattering and grain deviation
- High speed on chip image processing with 64 bit operating system

1.2.2 X-ray log scanner

As for another commercial product, X-ray log scanner from INRAY shown in **Figure 6**. This product is located outside, the main body is the component in grey color where all the measurement devices are included, the component in green color is the conveyor and its job is to transport the logs into the grey component. Then the scanning results can be transmitted to the computer software. It can also analyze the inner quality of the log and transfer the quality in an x-ray image. The log can be sorted based on the size and distributed to different usage. it does not occupy too much space and it requires minimum maintenance. The log is transported in one direction to the machine, the dimension and geometry data of the log are used to sort the logs, the x-ray images are generated immediately, the average that log pass the scanner is 0.2 seconds. (Inray.fi, 2019)

Figure 6. X-ray log scanner. (Inray.fi, 2019)

Some of the product features are listed as follow:

- The diameter of the heartwood can be measured
- The barkless diameter can be measured
- The branches or defects of the log can be detected
- The annual ring density of the log can be measured since it influences on several features of the products
- The x-ray shows the yields of the branchless parts of the log defined by the user
- The x-ray sorts the wood according to its external and internal features.

1.3 Importance of the vibration

In this section, the importance of the vibration will be mentioned. First part is some literature review about the vibration measurement, which helps to understand some physical and mathematic principle of vibration generation and vibration isolation. (Bonsel, Fey and Nijmeijer, 2004)

1.3.1 Vibration measurement method

There are several vibration methods in different fields. Here introduces some quite common and innovative method to measure the vibration, which are scanning laser doppler vibrometer, impact hammer test and 3D digital image correlation. (Dai et al., 2009, Zeng and Forssberg, 1994)

- Scanning laser doppler vibrometer

This kind of method is commonly used in the vibration filed to measure the velocity of the object surface. The reference beam is compared with the laser reflected from the object comes to sensor. And a relative shift can correlate to the surface velocity at the beams location. An illustration of the scanning laser doppler vibrometer can be seen in **Figure 7**. (Helfrick et al., 2011)

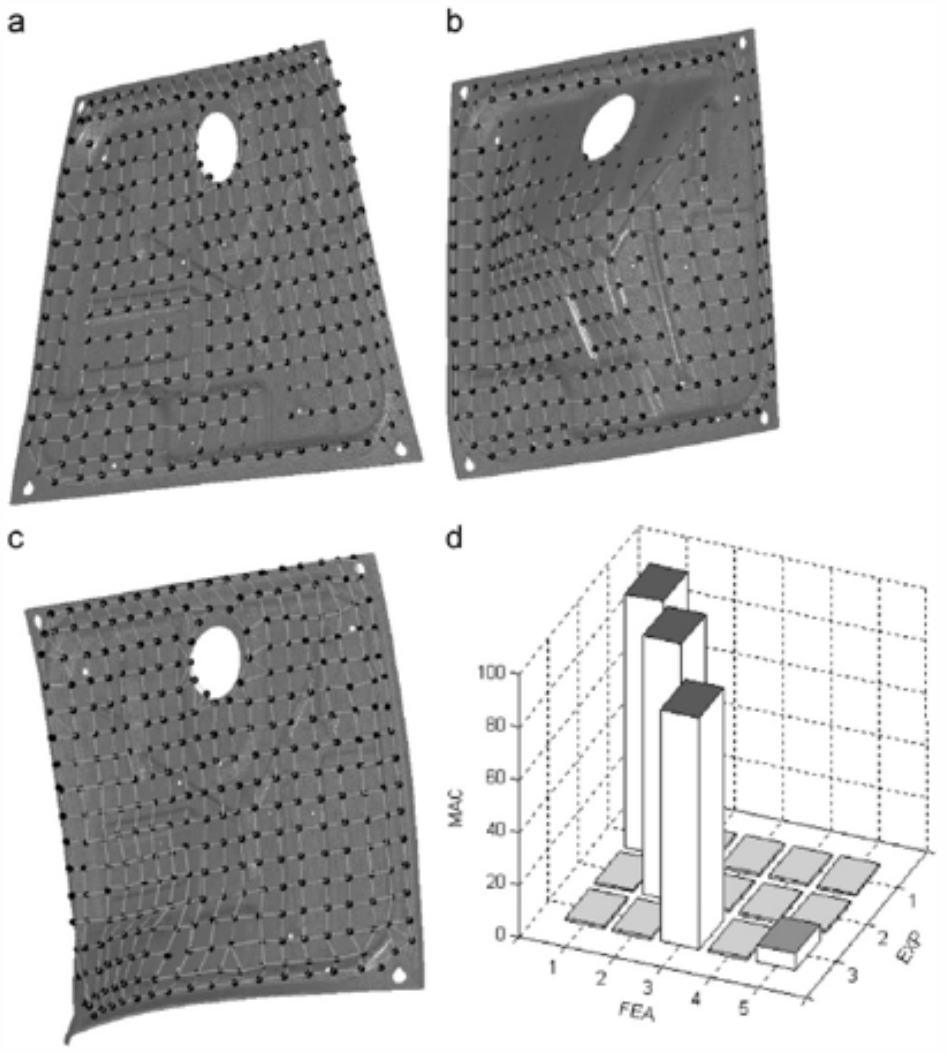

Figure 7. Scanning laser vibrometer test results. (Helfrick et al., 2011)

- Impact hammer test

The principle of the impact hammer test is impacting the structure under test with specific frequency, which will happen in infinitely short duration theoretically. The result of this test is constant amplitude in the frequency domain. During the test, duration of the time and frequency of the impact force are directly linked. And a special hammer with load cell on its tip is used to measure the force of the impact. To ensure the validation of the test, several

impact on several location the structure is required. An illustration of the impact hammer test can be seen in **Figure 8**. (Helfrick et al., 2011)

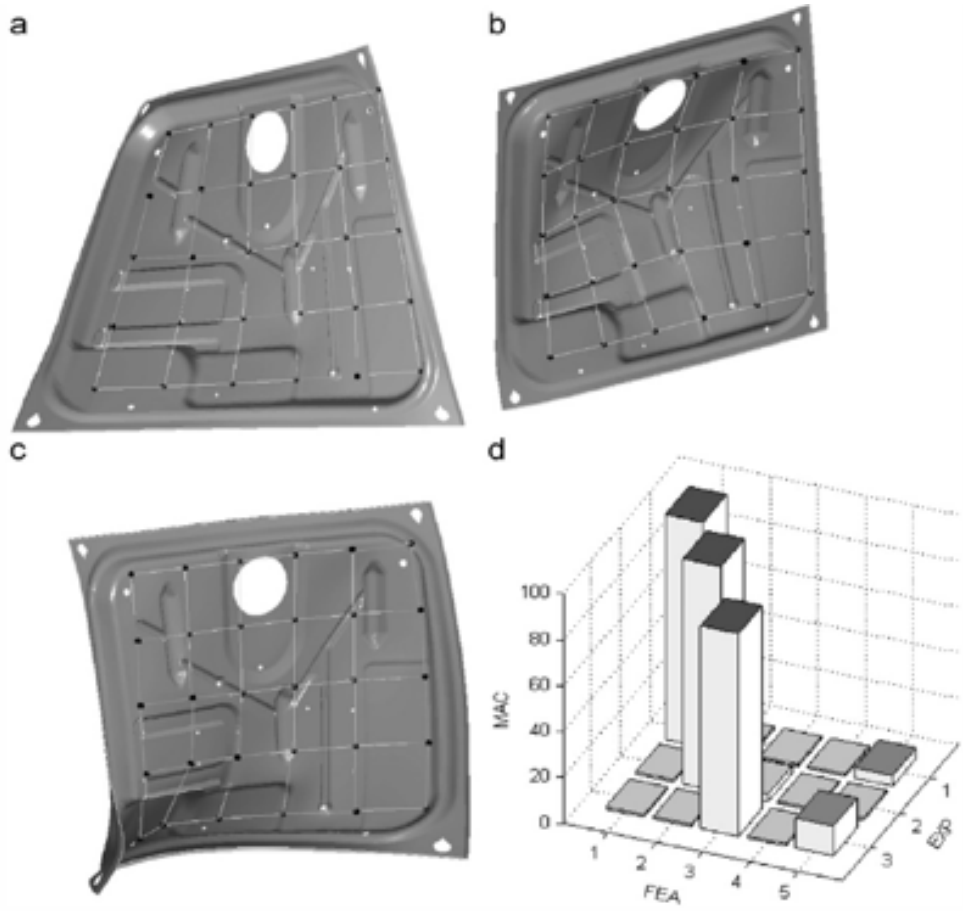

Figure 8. Impact hammer test results. (Helfrick et al., 2011)

- 3D digital image correlation

Differing from traditional vibration measurement methods, 3D digital image correlation is an innovative method that is applied in shape and deformation measurement of the structure. Compared with impact hammer test and scanning laser vibration meter, digital image correlation method is better on measurement of surface vibration and there are used for modal vector and shape information identification. Moreover, this method can provide abundant data in short response, therefore, it gives better geometric correlation with nodes in FE model compared to other method. (Helfrick et al., 2011)

The principle of this method can be seen in **Figure 9** and **Figure 10**. Digitized light intensity values across a rectangular array of pixels embedded in the CCD camera is the fundamental measurement principle. And a numerical gray-scale value related to the intensity of the light

reflected from the object is stored in each of the array cell. After the correlation process, the computer can recognize and track the unique point, which is defined by its surrounding information that involve light intensity and series of images. In the end, shape, displacement and strain of the tracked point can be measured.

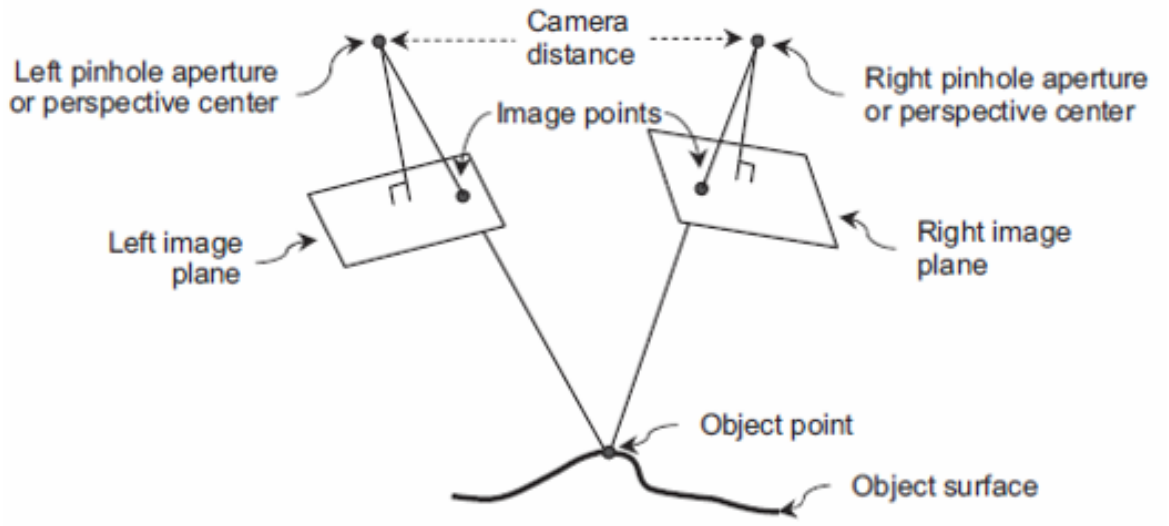

Figure 9. Principle of 3D digital image correlation method. (Helfrick et al., 2011)

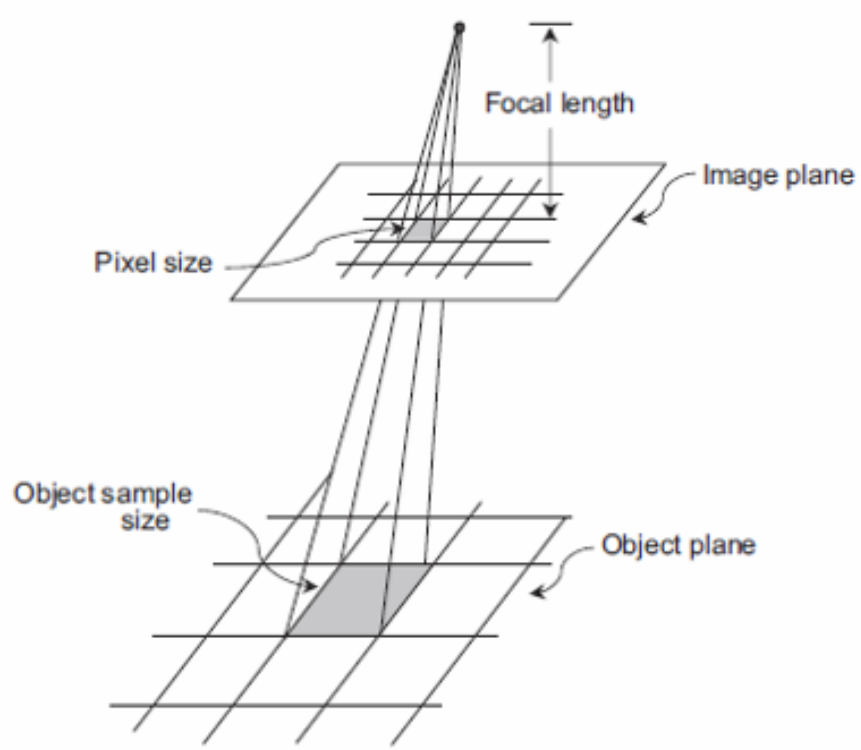

Figure 10. Pixel size in relation to object sample size. (Helfrick et al., 2011)

A comparison table between impact hammer test, scanning laser vibrometer and digital image correlation test can be seen in *Table 1*.

Table 1. Comparison between different laser measurement methods. (Helfrick et al., 2011)

IMPACT HAMMER TEST	DIC TEST	SCANNING LASER VIBROMETER
► Easy to obtain transfer functions	► Obtaining transfer functions requires post-processing beyond typical software capabilities	► Easy to obtain transfer functions
► Test each point separately	► Test each shape separately	► Test each point in series
► Data only at locations of response transducers	► Data on entire visible surface of an object	► Data at pre-defined points on visible surface of an object
► Sensitivity depends on accelerometer	► Sensitivity goes down as the field-of-view gets larger	► Sensitivity related to laser light wavelength
► Broadband excitation of all modes	► Better suited for single frequency excitation	► Broadband excitation of all modes
► No stability requirements	► Less sensitive to camera rigid body motion	► Calibration is highly sensitive to changes in setup conditions
► Inexpensive	► Expensive	► Very expensive
► Requires contact and possible mass loading	► Non-contacting and non-mass loading	► Non-contacting and non-mass loading
► Low spatial resolution	► Very high spatial resolution	► High spatial resolution

1.3.2 Vibration elimination applications

In this section, some mathematic and physical model to eliminate the vibration are introduced. These are the core principle of how the vibration of the object is removed and what the commercial vibration isolation device relies on. There are several models and method to explain the method of elimination of vibration, which are simple and easy to understand in this case. One is called tuned vibration absorber without damping and another one is vibration absorber with damping. When the inertia or elastic properties are the prior parameters that affect the object resonant frequency, the vibration absorber without damping is the preferred solution. (Deng and Gong, 2008, Jacquot, 1978, Templeton, 1993)

The tuned vibration absorber is illustrated in **Figure 11**. It is a system where a second mass m2 is connected to the primary mass m1 with spring of spring coefficient k2 and mass m1 is connected to the ground with spring of spring coefficient k1. (Noolvi, Raja and Nagaraj, 2017)

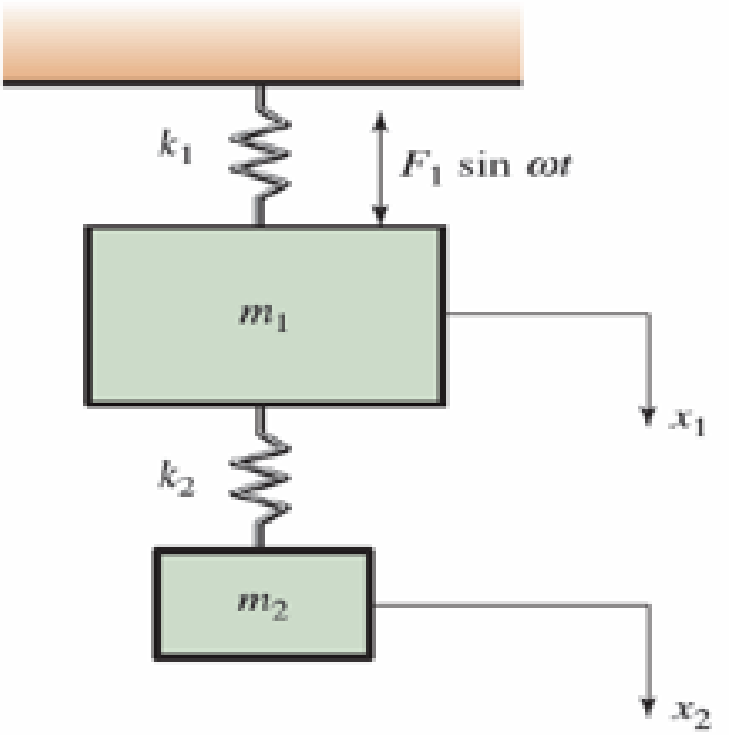

Figure 11. Tuned vibration absorber without damping. (Noolvi, Raja and Nagaraj, 2017)

The equation of motion can be expressed as:

$$x_1 = A sin\omega t \quad (1)$$

$$x_2 = B sin\omega t \quad (2)$$

$$A = \left(\frac{F_1}{k_1}\right)\left[\frac{1-\left(\frac{\omega}{\omega_2}\right)^2}{\left(1+\mu\left(\frac{\omega_2}{\omega_1}\right)^2-\left(\frac{\omega}{\omega_1}\right)^2\right)\left(1-\mu\left(\frac{\omega}{\omega_2}\right)^2\right)-\mu\left(\frac{\omega_2}{\omega_1}\right)^2}\right] \quad (3)$$

Where:

$$\omega_1 = \sqrt{\frac{k_1}{m_1}} \quad (4)$$

$$\omega_2 = \sqrt{\frac{k_2}{m_2}} \quad (5)$$

ω_1 and ω_2 are the natural frequencies of the system and absorber.

When the external force frequency is equal to the natural frequency ω_2, the mass will not vibrate at all. So, the elimination of the vibration is achieved by adjusting mass and spring constant to let $\omega_1 = \omega_2$.

If the damper or tuned mass damper is taken into consideration as shown in **Figure 12**. Compared to the tuned vibration absorber without damping, a dashpot β is added. However,

it can eliminate the vibration based on viscous vibration absorber. It is not as effective as the tuned mass dampers.

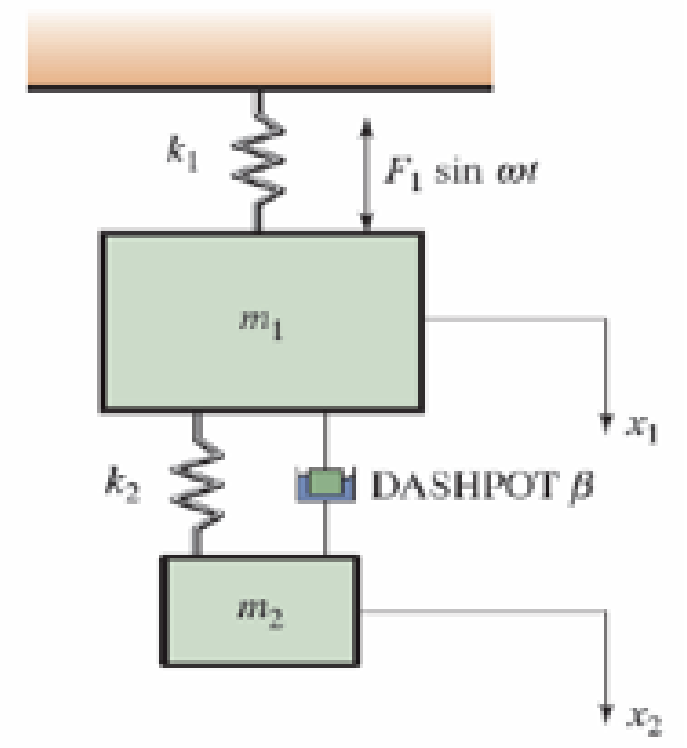

Figure 12. Vibration absorber with damping. (Noolvi, Raja and Nagaraj, 2017)

The equation of motion can be expressed as:

$$x_1 = Asin(\omega t + \varphi_1) \quad (6)$$

$$x_2 = Bsin(\omega t + \varphi_2) \quad (7)$$

1.4 Temperature fluctuation in 3D and X-ray measurement

There are several scanning devices integrated in the machine, such as X-ray camera and laser camera, when these machine works, they generate heat. Then the heat can radiate and induct to the aluminum frame and plates. Due to the temperature changes, the aluminum frame will have deflection and decrease the accuracy of the scanning. Except the heat generated from inside the machine, the external environment is another parameter affect the temperature fluctuation. During the design phase, the deformation of the aluminum frame is considered when the temperature changes from 30℃ to -30℃, which can be the average temperature outside during summer and winter. (Liu et al., 2006, Zhou, Jeffries and Hanson, 2005)

1.4.1 Temperature fluctuation in structure

When the temperature of aluminium alloy is increased, the metal will expand, and it is also called thermal expansion. For example, take aluminium alloy 6063 as an example, when the temperature is -20°C, the length is 2700 mm long. When the temperature increases to 30°C, the length of the aluminum alloy increase to be 2703 mm due to thermal expansion. A picture shows above situation and is shown in **Figure 13**. (Alumeco.com, 2019)

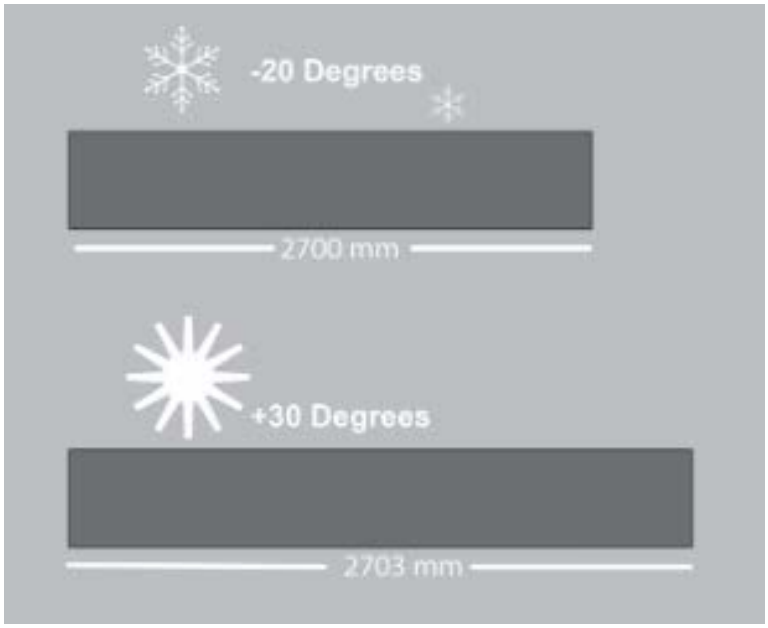

Figure 13. Thermal expansion. (Alumeco.com, 2019)

1.4.2 Temperature insulation

Since the temperature fluctuation will result structure deformation and lead to serious problem such as structure breakdown, which further cause radiation leakage and harm human health. In safety respect, temperature insulation is required. However, it is important to know how heat is transferred in the structure, to be more specific, how the heat is transferred between different material layers in extreme temperature of the design. The main heat transferred method is conduction, convection and radiation. In this case, we assume the heat conduction is the only heat transfer method since others are quite few in our consideration.

The heat conduction is described as the heat energy is transferred through gas, liquid, gas or other kinds of material. Different from heat convection and heat radiation, there is physical contact between structures, or layers in our case. It is true that all of these three modes of

heat transfer existed, but the heat conduction through walls, floors and windows are the most significant one. Details of thermal conduction will be introduced in following section in which related physical symbols and formula are listed and introduced in detail.

After some definition of heat insulation introduced above, here tells why the insulation is necessary. The insulating is achieved by put different insulating materials between environment and the objective. There are several popular insulating materials and the desirable characteristics for insulation materials are listed below: (Biesmans et al., 1998, Demharter, 1998, Tseng, Yamaguchi and Ohmori, 1997)

- Thermal conductivity
  This thermal conductivity should be as low as possible as good insulation material.

- Moisture-vapour permeability
  This moisture-vapour permeability should be as low as possible as well as good insulation material, it means almost negligible water absorption and minimized condensation and corrosion.

- Resistance and installation features
  The material of insulation should resist water, chemicals and solvents in the specific situation and durable. Another characteristic should be adhesive to other material since mostly, there will another layer installed outside the insulation material to have a acceptable appearance.

- Safety features
  The material should be safe in manner of nonexplosive, nonflammable or cause other hazards.

2 METHOD

In this chapter, the methods of measuring the vibration and the temperature will be introduced.

2.1 Vibration measurement

One of the most common methods for measuring vibration is the use of vibrometer and the aim is to know the vibration around the device area, because the vibration has significant effect on the measurement. The collected data can be charted and guide for choosing suitable vibration pad since the level of vibration is related to the balance, assembly of each components. High level of vibration may cause by misalignment and poor balance. The vibration data can be measured using vibrometer shown in **Figure 14**. However, here the software on mobile phone can just be used to collect the data. The reason of choosing this method is due to its feasibility and cost-efficience and this function is quite mature already. By checking the corresponding natural frequency at the amplitude. The vibration pad can be found based on the machine itself parameters, such as weight and the size. The collected data can be seen in following section. (Lionprecision.com, 2019)

Figure 14. Vibrometer. (Mmf.de, 2019)

2.2 Temperature fluctuation

As for the aluminum structure, there will be contraction and expansion of the structure changes when the temperature fluctuates in Finland. The cube will be put in the environment between - 30℃ to 30℃ after consideration of Finland temperature outside and inside as well as transportation process. The aluminum frame can be seen in **Figure 15**. The aluminum frame is covered by plate, there are inner temperature sensor equipped inside the container and outside temperature sensor equipped outside the container so that both of the temperature data of the container inner and outer surface temperatures can be recorded, which is important in our temperature system because the temperature difference will cause some changes on the structure and it further influences the measurement accuracy. Solidworks is used to model. (Solidworks.com, 2019)

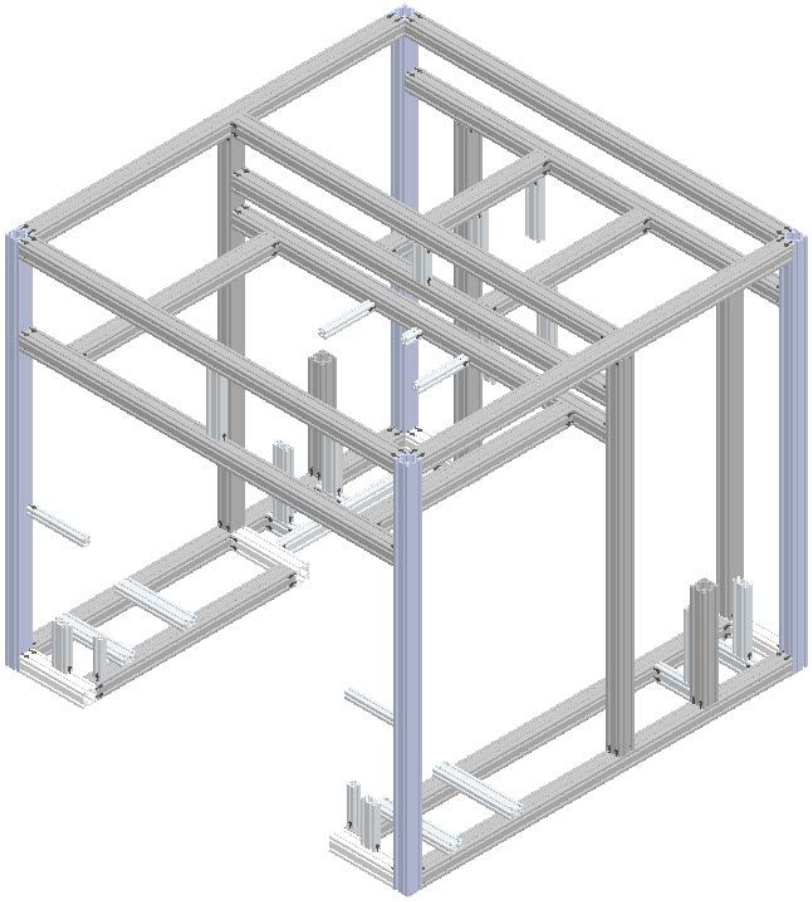

Figure 15. The aluminum frames.

The method for estimation and simulate the temperature effect on frame is by using commercial software. The FE analysis of the aluminum frame is carried out, due to high complexity of the aluminum structure, the analysis cannot done by using Ansys workbench

with education license. Instead, only one aluminum beam shown in **Figure 16** is analyzed with automatic meshing setting, one side of the beam is fixed supported, two set of FE analysis settings are used. In the first set, the original temperature is 20℃ and the end temperature condition is -20℃. In another set, the original temperature is 30℃ and the end temperature condition is -30℃. The results will be mentioned in the next chapter.

Figure 16. Aluminum beam.

As for temperature control, the collected data will be sent to the control program and the system will decide if the temperature control system works or not, here the air pump is adopted to control the temperature. And the temperature is controlled around 20℃. To select the suitable air pump, basic calculation of heat loss is carried out, in the design, the parameters of each structure, such as floor, wall and windows are measured based in mechanical aspects. The exact parameters can be seen in *Table 2*.

Table 2. Parameters of the insulation structure.

	Floor	Wall	Tunnel	Ceiling	windows	Doors
Sizes	2 floors 2500x1000	2 walls 3000x2400	2500x3800	3000*2500	700x600 700x600 500x400 500x400 500x400	4 doors 2000*900
Glass					3mm	
Plywood	20mm					
Epoxy zinc rich primer		30 mic	30 mic	30 mic		30 mic
Epoxy primer		40 mic	40 mic	40 mic		40 mic
Acrylic top coat		40 mic	40 mic	40 mic		40 mic
Steel		2.5	2.5	2.5		1.5mm
Cardboard+Air						40mm
Steel						1mm
Epoxy zinc rich primer		30	30	30		30mm
Closed cell PU	66mm	70mm	50mm	70mm		40mm
lead	3mm	3mm	3mm	3mm		3mm
plywood	15mm	15mm	9mm	15mm		6mm
Acrylic top coat	100mic	100mic	100mic	100mic		100mic

Figure 17 shows unfinished structure surface, the coarse material on the surface is PU material, which is the first layer of the cube, outside is steel, the PU material is further grinded and covered by 3mm lead to assure the safety and finally by plywood, the final structure is shown in **Figure 18**.

Figure 17. PU coating on cube.

Figure 18. Plywood on cube.

A variety of methods are used to calculate the heat loss. This paragraph introduces one of the method of heat loss calculation applied in this study. Starts from basic terms definitions: (Fao.org, 2019)

- Heat energy

  1 kcal is the amount of heat or energy needed to raise the temperature of 1 kg of water by 1 degree Celsius. The unit of energy is J.

- Thermal conductivity

  Thermal conductivity is a measure of the capacity of a material to conduct heat through unit area of unit thickness of material in a unit temperature difference. It is known as k value.

- Coefficient of thermal conductance

  The coefficient of thermal conductance is defined as the amount of heat conducted in 1 hour through 1 m^2 of material with 1 m thickness in 1 degree Celsius temperature differences.

- Thermal resistance

  The thermal resistance is known as R value and defined as the resistance that material offers to the heat flow. Good insulating material has high R value.

- Coefficient of heat transmission

  The coefficient of heat transmission is known as U, it includes the all the thermal resistance of conducted surface.

There are wide range of good insulation materials, such as polyurethane foam, expanded polystyrene, expanded perlite, fiberglass and cork. A common insulating material are listed below in *Table 3*:

Table 3. Comparison between different insulating materials. (Fao.org, 2019)

Insulating material	R value per inch	Advantages	Disadvantages
Polyurethane, board	6.25	Very good R-value, can be used with fiberglass resins	Not always easily available, relative expensive
Polyurethane, spray on	7.0	Very good R-value, can be used with fiberglass resins, easy application with spray equipment	Not always easily available, expensive, requires special spray equipment
Polyurethane, poured (two-part chemical)	7.0	Very good R-value, can be used with fiberglass resins, relative ease of application	Not always easily available, expensive, requires very careful volume calculations
Polystyrene, sheets (smooth) Trade name "Styrofoam"	5.0	Readily available, low cost, reasonable R-value	Cannot be used with fiberglass resins unless protected, easily damaged
Polystyrene foamed in place and expanded molded beads. Known as Isopor, Polypor, etc.	3.75-4.0	Reasonable R-value, lower cost than smooth surfaced sheets	Cannot be used with fiberglass resins unless protected, easily damaged
Cork board	3.3	Availability in many markets, reasonable cost, can be covered with fiberglass	Low R-value than polyurethane for styrene foams
Fiber glass wool batts	3.3	Low cost, ease of installation	Readily absorbs water or other fluids, loses insulating value when wet
Rock wool batts	3.7	As above	As above
Wood shavings	2.2	Readily available, low cost	Absorbs moisture and loses R-value when wet, decays
Sawdust	2.44	Readily available, low cost	Absorbs moisture and loses R-value when wet, packs down under vibration
Straw		Readily available, low cost	Absorbs moisture and loses R-value when wet, host to insects, etc.
Air space	Approx. 1.0	No cost	Has to be completely sealed to prevent air circulation causing heat infiltration

From the above table and from the market commercial product, here we select closed cell polyurethane in our application.

Since the calculation involves multi-layer wall, all the walls or materials should be calculated separately and be summed together in a way, the main formulas 1 and 2 are: (Engineeringtoolbox.com, 2019)

$$\frac{1}{UA} = \frac{1}{h_{ci}A_i} + \sum \frac{s_n}{k_n A_n} + \frac{1}{h_{co}A_o} \quad (1)$$

Where:

U: The overall heat transfer coefficient (W/(m^{2}K))

A: Wall area (m^2)

$h_{c,i,o}$: Inside or outside wall individual fluid convection heat transfer coefficient (W/(m^{2}K))

s: Thickness of layer (m)

k: Thermal conductivity of material (W/(mK))

The heat transfer calculation is shown in formula 2

$$q = UAdT \quad (2)$$

Where:

q: Heat transfer (W)

dT: Temperature difference

3 RESULTS

This chapter is divided into two parts to tell the results of the vibration measurement and temperature measurement.

3.1 Vibration

In the vibration measurement, we get the data in txt file, and we curve them in Excel sheet. Through the measurement. There are four sets of data collected that are enough for us to choose suitable vibration isolation device. The figures are illustrated separately in **Figure 19**, **Figure 20**, **Figure 21** and **Figure 22**, which are made in Excel from table to graph.

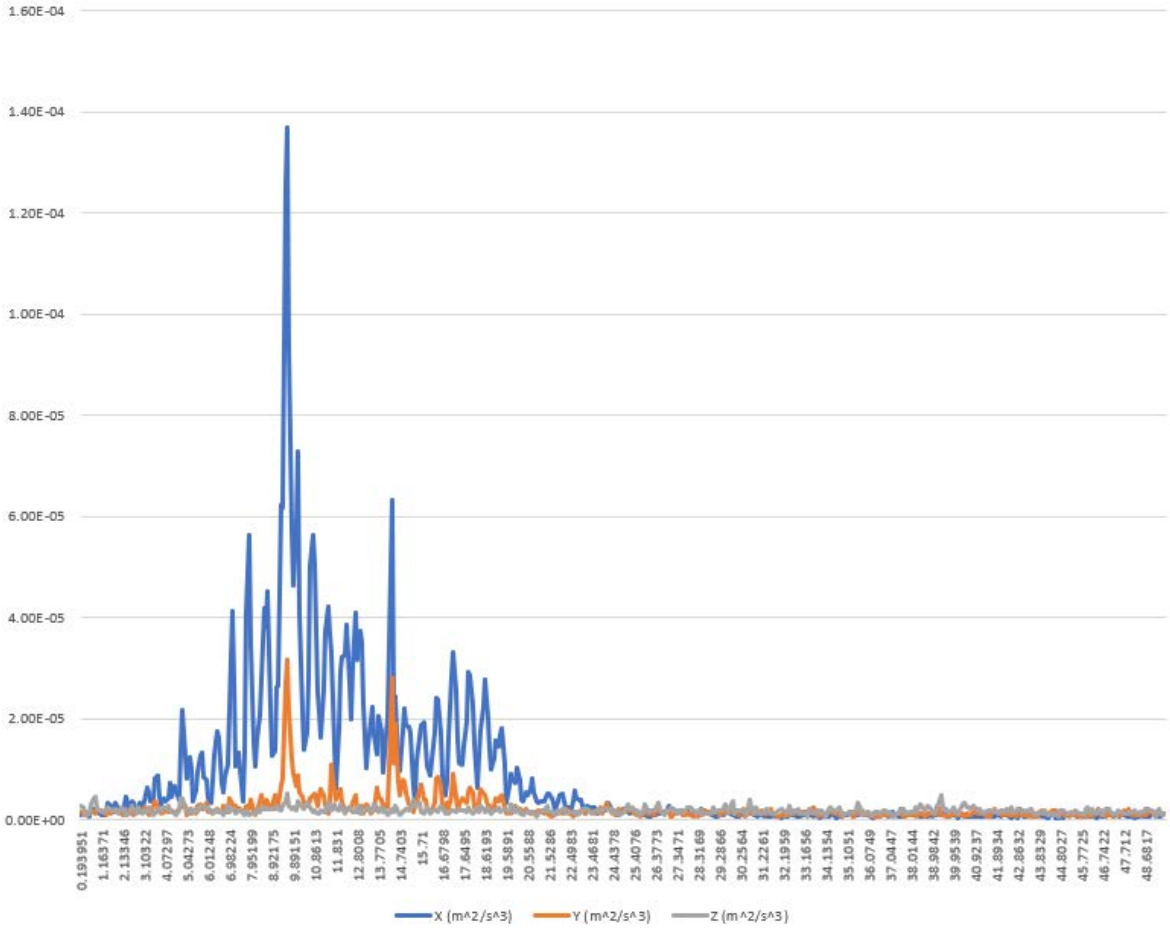

Figure 19. Vibration measurement data 1.

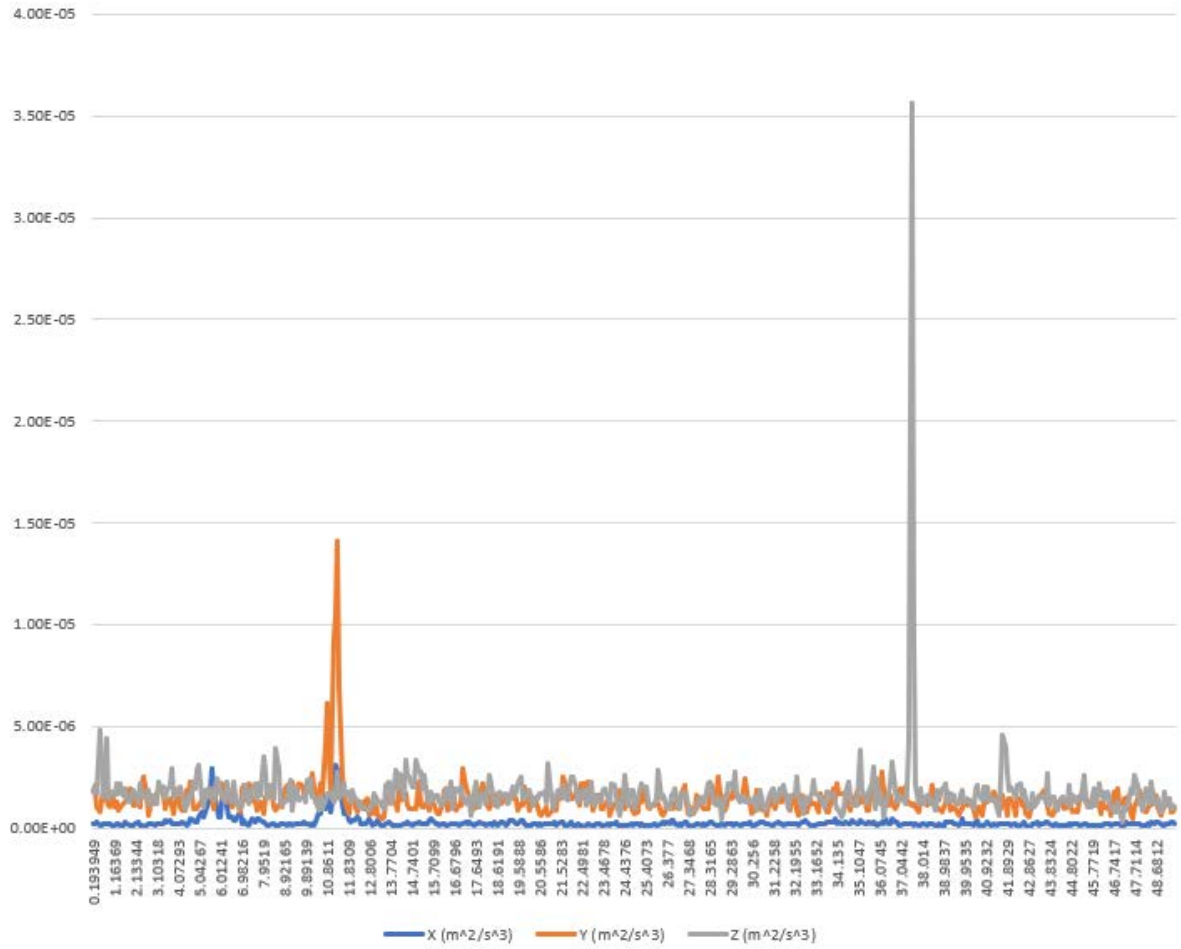

Figure 20. Vibration measurement data 2.

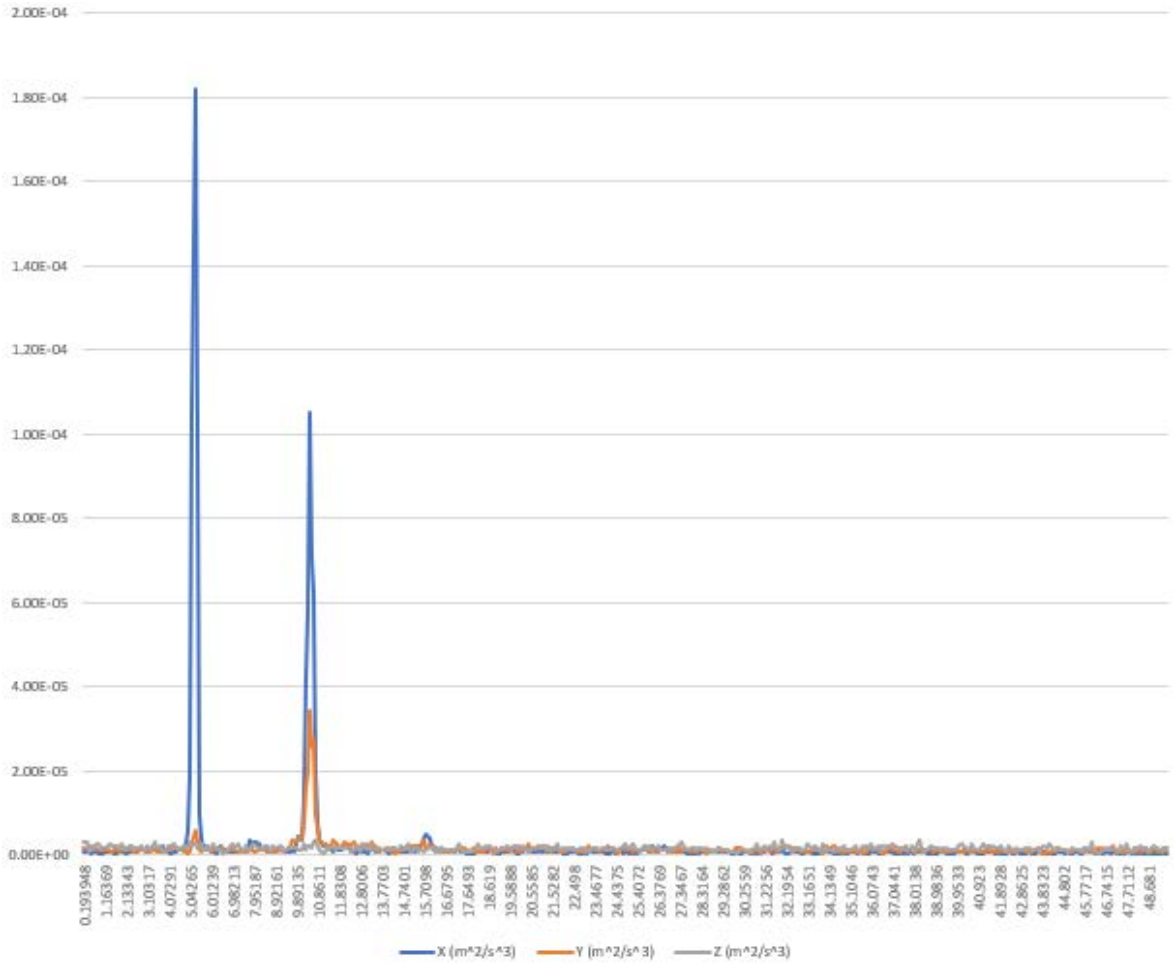

Figure 21. Vibration measurement data 3.

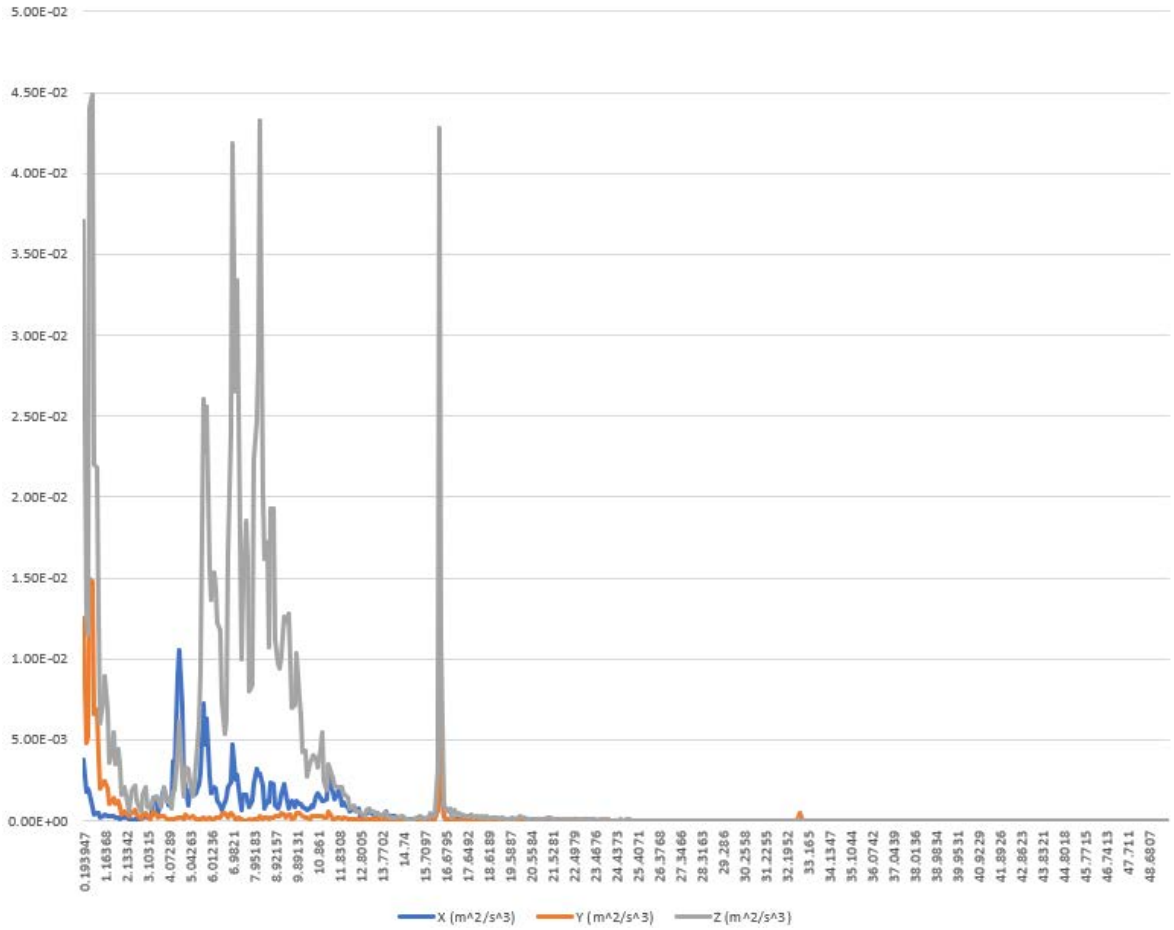

Figure 22. Vibration measurement data 4.

3.2 Vibration isolation device.

The selected vibration isolation device is called RAEM shown in **Figure 23**, which is suitable for both light and heavy machines. The geometry of the RAEM can be seen in **Figure 24** and the type of the RAEM can be seen in *Table 4*. The detail selection procedure comes in the following.

Figure 23. RAEM mountings. (Costa, 2013)

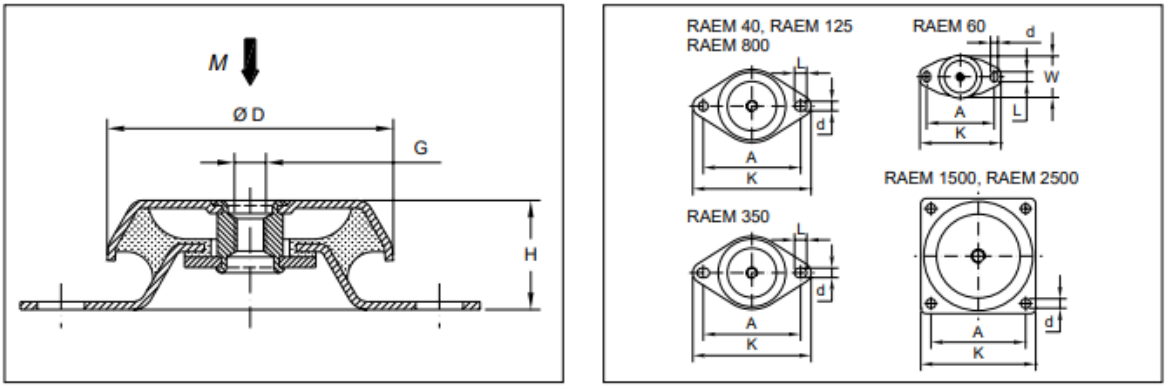

Figure 24. Technical drawing of RAEM. (Costa, 2013)

Table 4. Type of different RAEM. *(Costa, 2013)*

Type	Art.No. 40° IRH	Art.No. 60° IRH	Dimensions in mm D	A	W	H	K	d	L	G	Weight (kg)	*M*-Max(kg) 40° IRH	60° IRH
RAEM 40	1861860	1861870	64	88		35.5	110	9	12	M10	0.26	30	60
RAEM 60	2256760	2256770	63	100	61	35.5	120	11	15	M12	0.30	60	120
RAEM 125 M10	1861720	1861730	84	110		35.5	135	11	15	M10	0.37	80	180
RAEM 125 M12	2256140	2256150	84	110		35.5	135	11	15	M12	0.37	80	180
RAEM 350 M12	2256440	2256450	110	140-148		42	175	14	18	M12	0.80	200	400
RAEM 350 M16	1861780	1861790	110	140-148		42	175	14	18	M16	0.80	200	400
RAEM 800	1861840	1861850	155	182		54	216	14	18	M16	1.8	450	800
RAEM 1500	2255400	2255410	182	146		85	180	14		M20	3.0	900	1700
RAEM 2500	2255420	2255430	224	180		105.5	220	17.5		M24	4.6	1700	3400

The product is selected based on *Table 4* and **Figure 25** given by the manufacturer. First of all, the vibration absorber is chosen based on the relation between amplitude and natural frequency shown in **Figure 19**, **Figure 20**, **Figure 21** and **Figure 22**. From **Figure 19**, the natural frequency corresponding to the highest amplitude is between range 6 Hz – 10 Hz. From **Figure 20**, the natural frequency corresponding to the highest amplitude is between range 8 Hz – 11 Hz, as for the peak around 38Hz, it might be caused by the outside disturbance since the change is so sudden only in z direction. From **Figure 21**, the natural frequency corresponding to the highest amplitude is between range 4 Hz – 6 Hz and 8 Hz – 10 Hz, however, the natural frequency between 8 Hz – 10 Hz is more valuable since the trend between x and y direction are the same. From **Figure 22**, the natural frequency corresponding to the highest amplitude is between range 0 Hz – 2 Hz, 6 Hz – 10 Hz and 15 Hz – 16 Hz, this set of data might not be good, the reason can be the disturbance at the beginning and outside disturbance. As a result, the natural frequency corresponding to the highest amplitude is between range 8 Hz – 10 Hz. The type of the model chosen is RAEM2500 10-00160. And the selected model parameter can be seen in *Table 5*.

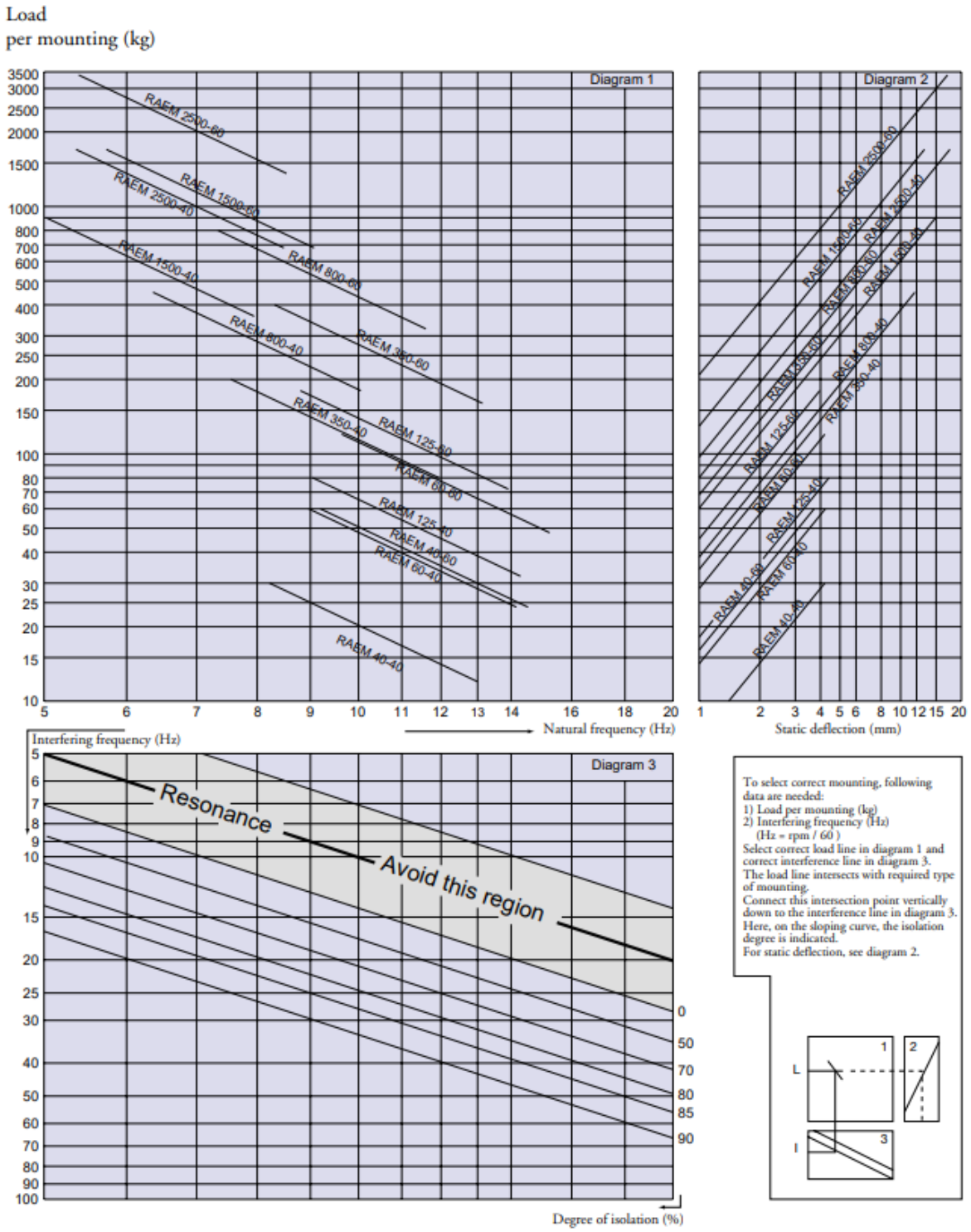

Figure 25. Graph used to choose suitable product. (Costa, 2013)

Table 5. Technical parameter of RAEM.

D	A	H	K	D	G	M-max	Weight
224	180	105.5	220	17.5	M24	1700	4.60

The vibration pad installed in the machine can be seen in **Figure 26**, which shows the installation process. There are four vibration pads in total and they are located separately in the four corners of the cube.

Figure 26. Vibration pad installation.

3.3 Temperature fluctuation

The aluminum structure in the workplace can be seen in **Figure 27**. The black box is the place where all the measurement and scanning components placed, they must be sealed safely to avoid dangers from the laser beam and X-ray.

Figure 27. Aluminum frame in the cube.

In the first data set, the temperature fluctuates from 20℃ to -20℃. The total deformation and the equivalent stress of the frame can be seen in **Figure 28** and **Figure 29**. Ansys workbench is used to simulate. (Anon, 2019)

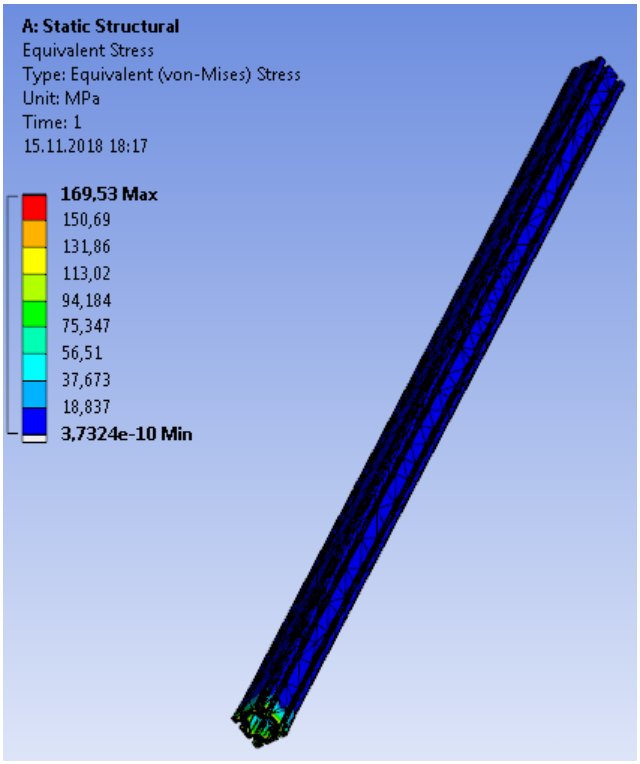

Figure 28. The equivalent stress of the beam in set 1.

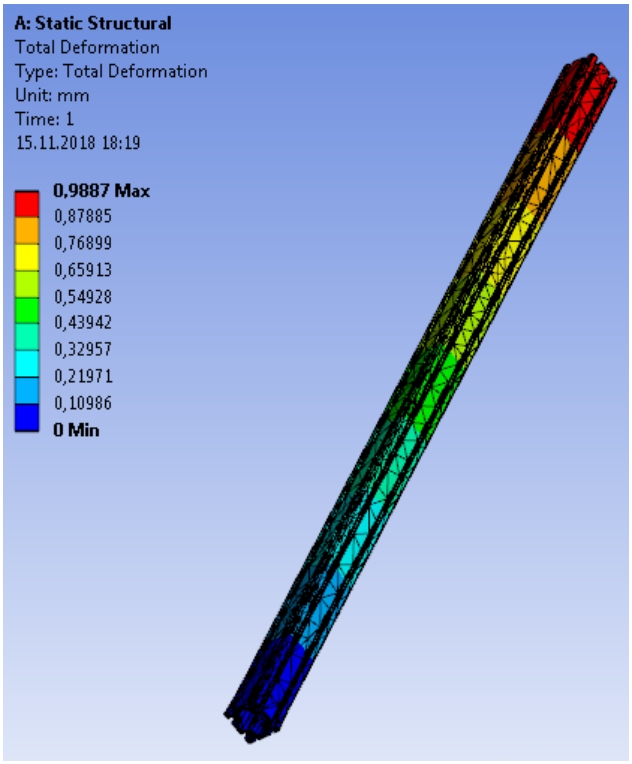

Figure 29. The total deformation of the beam in set 1.

In the second set, the temperature fluctuates from 30°C to -30°C, the total deformation and the equivalent stress can be seen in **Figure 30** and **Figure 31**.

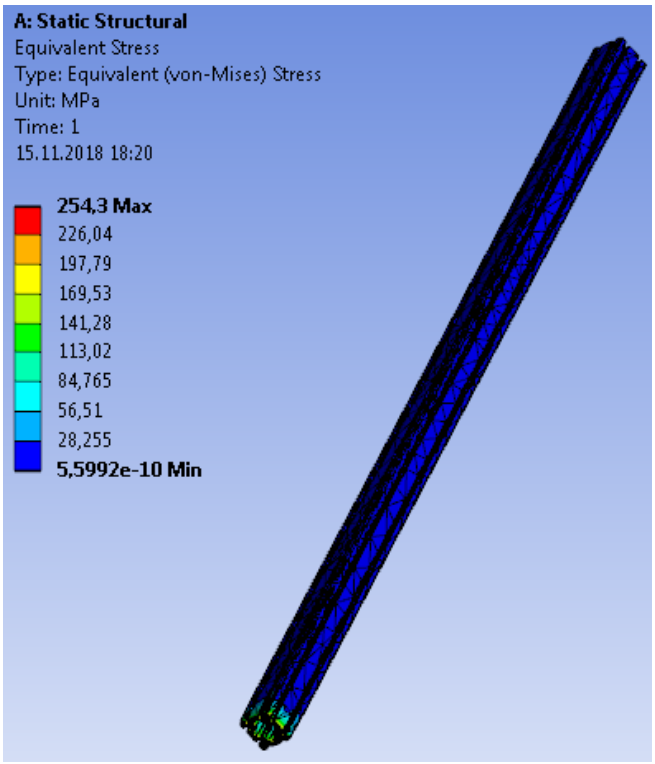

Figure 30. The equivalent stress of the beam in set 2.

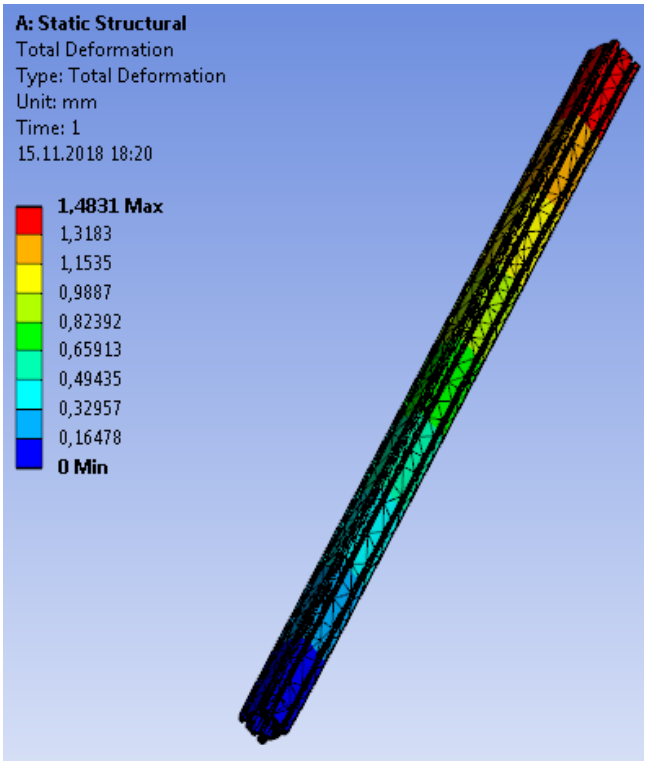

Figure 31. The total deformation of the beam in set 2.

From the FE analysis results, the deformation of the beam is around 1 mm to 1.5 mm, which are extreme dangerous in industrial application, because this amount of deformation applied on stiffness steel structure, it causes structure breakdown. And the equivalent stress is high but under the material properties. However, this structure is a cubic structure and the analysis here is only one beam. It is obvious that the whole structure has high stiffness than this single beam.

From *Table 2*, we get the parameters of each layers, by using the formula 1, we get the heat loss in each layer when the suggested extreme temperature of environment is between -50℃ and 20℃. There are different materials in each layer, wall areas are shown in previous table, the thermal conductivity of material in layers are shown in *Table 6*.

Table 6. Thermal conductivity of each materials at 25℃. (Engineeringtoolbox.com, 2019)

	Thermal conductivity (W/(mK))
Plywood	0.13
Closed cell PU	0.03
Lead	35
Acrylic top coat	0.2

Epoxy zinc rich primer	0.35
Epoxy primer	0.35
Steel	17
Glass	1.05
Cardboard and air	0.02

The heat conductivity coefficient calculated by using formula 1 is shown in *Table 7*.

Table 7. Heat conductivity coefficient in multi-layer structure.

	Heat conductivity (W/(mK))
Floor	0.191
Wall	0.192
Tunnel	0.491
Ceiling	0.364
Windows	3.279
Doors	0.072

The Heat transfer calculated by using formula 2 can be seen in *Table 8*. Here the temperature fluctuation is assumed to be from -50℃ to 25℃.

Table 8. Heat transfer in each layer of the cube.

	Heat transfer (W)
Floor	33.425
Wall	97.272
Tunnel	326.515
Ceiling	191.1
Windows	82.631
Doors	9.072
Total	740.015

After the calculation, the suitable air pump Mitsubishi MSC-LN 25 air heat pump is selected, which is shown in **Figure 32**. It provides full rated heating capacity down to -15℃ and guaranteed heating operation down to -25℃, so even in Finland, it will work properly since the devices inside will generates heat. (Mitsubishi-electric.co.nz, 2019)

Figure 32. Mitsubishi MSC-LN 25 air heat pump. (Mitsubishi-electric.co.nz, 2019)

From the real situation temperature measurement. The data collected is plotted in excel and shown in **Figure 33**. The finnosPlc_TemperatureOutside marked with yellow color shows the room temperature or environment temperature and it fluctuates within the time in the day. The fluctuation on temperature is what we need to avoid, so air pump is adopt in the cube and temperature control results can be seen in the figure as well. The curve finnosPlc_TemperatureContainerDown marked as blue and finnosPlc_TemperatureContainerUp marked as grey are the results we are looking. As we can see here, the curve is relatively flat compared to the room temperature, which means the temperature is under control. The selected temperature devices will shown in next section.

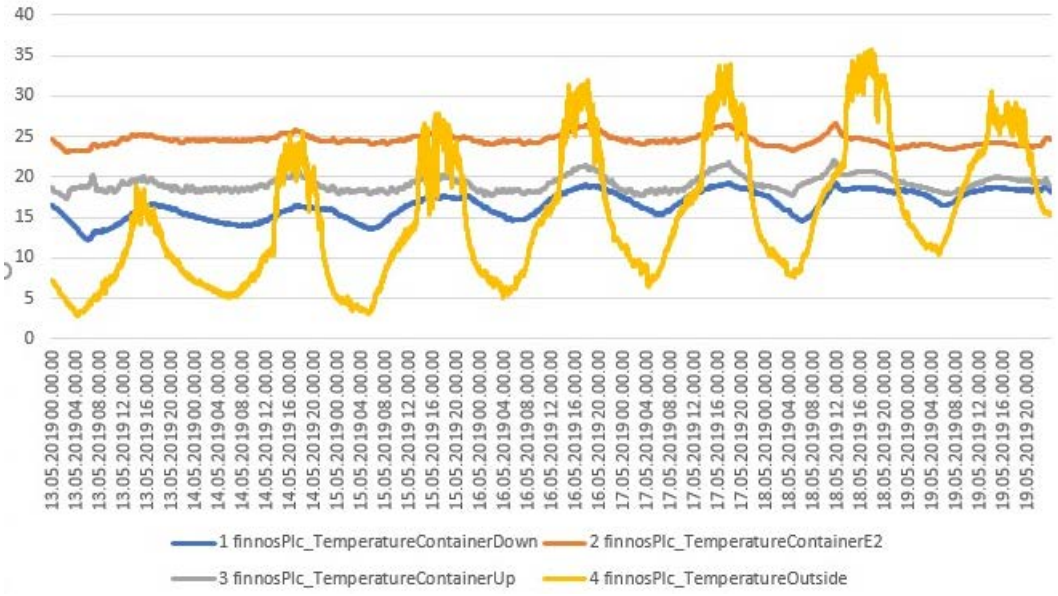

Figure 33. Temperature in the cube.

3.4 Selected temperature control device

There are two different temperature sensors that are used, they are connected to our logic controllers. The model connect to our inside container is ATF-1 as shown in **Figure 34** and the model connect to our outside container is ATF-2 as shown in **Figure 35**. These sensors can be used to measure outside temperatures and in wet room areas as well. Some technical data can be seen in **Figure 37**. One of the temperature sensors is marked by red circle in **Figure 37**. Due to some company confidential issues, some part of the figure is hidden. (S+S Regeltechnik, 2019)

Figure 34. ATF-1. (S+S Regeltechnik, 2019)

Figure 35. ATF-2. (S+S Regeltechnik, 2019)

Figure 36. Temperature sensor.

TECHNICAL DATA	
Measuring range:	-50...+90 °C
Sensors / output:	passive (see table), **ATF01 sensors internal** **ATF1 sensors internal** **ATF2 sensor inside external sensor tube** made of stainless steel, 1.4571, V4A
Connection type:	2-wire connection (4-wire connection on PT100/PT1000A, optional on other sensors)
Testing current:	approx. 1 mA
Enclosure:	plastic, UV-stabilised, material polyamide, 30 % glass-globe reinforced, colour traffic white (similar to RAL 9016), **ATF01 with snap-on lid,** **ATF1 with quick-locking screws,** (slotted / Phillips head combination) **ATF2 with quick-locking screws,** (slotted / Phillips head combination)
Enclosure dimensions:	72 x 64 x 37.8 mm (Typ 1 / Typ 01)
Cable gland:	M 16 x 1.5; including strain relief, exchangeable, max. inner diameter 10.4 mm
Electrical connection:	0.14 - 1.5 mm² via terminal screws on circuit board
Insulating resistance:	≥ 100 MΩ, at +20 °C (500 V DC)
Humidity:	< 95 % r. H., non-precipitating air
Protection class:	III (according to EN 60730)
Protection type:	**ATF01 IP 43** (according to EN 60529) **ATF1 IP 65** (according to EN 60529) **ATF2 IP 65** (according to EN 60529)
Optional:	with sunshade **SS02** (ATF2, available on request)

Figure 37. Technical data of temperature sensor. (S+S Regeltechnik, 2019)

4 CONCLUSION

Returning to the question posed at the beginning of this thesis work, it is now to state that the vibration and temperature control are solved by selecting suitable vibration pad and temperature control devices. In this practical thesis, the circumstantial factors affecting on the measuring accuracy was studied and some experimental data was gathered from a commercially used Finnos scanner.

First the different type scanners on market was reviewed. All scanners (except Finnos) is at least semi open structure (cold air gets inside the scanner through the conveyor tunnel), which cause thermal expansion (or shrinking) in the scanner frame.

The phenomena of mechanical vibration were studied. Experimental data was examined before and after using a vibration damper. The results show that the choosing of a correct vibration damper will reduce the mechanical vibration to an acceptable level.

Thermal expansion was studied on an aluminum piece. Total expansion was 3mm for 2700mm aluminum beam. A study for overall effect on the expansion for complex frame structure was not carried out. However, in case there is 3mm expansion in each 2700mm beam the expansion in the frame is nonlinear, because the are beams of several lengths, interfaces (aluminum to plastic) and mountings (steel, aluminum, plastic). It means that every measuring component installed to the frame will change its position nonlinearly with respect to the temperature (thermal expansion). Therefore, when a system is calibrated it is calibrated in only on the temperature during calibration. When the temperature is changed the system is no longer calibrated and the measuring results from the scanner are no longer accurate. The Finnos scanner was equipped with an air-conditioning system and the experimental results show that the electrical cabin inside the scanner is independent of the outside temperature.

The work shows how the circumstantial factors such as vibration and temperature fluctuation can be cancelled out to ensure accurate scanning in online scanning systems such as in

Finnos Log scanner. These finding raised important practical issues that have a bearing on the similar log scanner product. Although this study focuses on our own product, the finding may well adopt in other similar products

LIST OF REFERENCES

Siltanen, S., Kolehmainen, V., J rvenp, S., Kaipio, J., Koistinen, P., Lassas, M., Pirttil, J. and Somersalo, E. (2003). Statistical inversion for medical x-ray tomography with few radiographs: I. General theory. Physics in Medicine and Biology, 48(10), pp.1437-1463.

Mendoza, A., Roininen, L., Girolami, M., Heikkinen, J. and Haario, H. (2019). Statistical methods to enable practical on-site tomographic imaging of whole-core samples. GEOPHYSICS, 84(3), pp.D89-D100.

Oy, F. (2019). Finnos | The Era of X-Ray Is Here.. [online] Finnos.fi. Available at: https://www.finnos.fi/en/ [Accessed 2 Jan. 2019].

Microtec.eu. (2019). Goldeneye 500 / Microtec. [online] Available at: https://microtec.eu/en/catalogue/products/goldeneye500/ [Accessed 2 Jan. 2019].

Inray.fi. (2019). [online] Available at: http://www.inray.fi/data/Inray_Log_EN.pdf [Accessed 2 Jan. 2019].

Noolvi, B., Raja, S. and Nagaraj, S. (2017). Actively Tuned Vibration Absorber using Smart Adaptive Composites. Materials Today: Proceedings, 4(2), pp.3506-3512.

Helfrick, M., Niezrecki, C., Avitabile, P. and Schmidt, T. (2011). 3D digital image correlation methods for full-field vibration measurement. Mechanical Systems and Signal Processing, 25(3), pp.917-927.

Alumeco.com. (2019). Temperature effects on aluminium items |. [online] Available at: https://www.alumeco.com/knowledge-technique/general/thermal-expansion [Accessed 2 Jan. 2019].

Biesmans, G., Mertens, A., Duffours, L., Woignier, T. and Phalippou, J. (1998). Polyurethane based organic aerogels and their transformation into carbon aerogels. Journal of Non-Crystalline Solids, 225, pp.64-68.

Demharter, A. (1998). Polyurethane rigid foam, a proven thermal insulating material for applications between +130°C and −196°C. Cryogenics, 38(1), pp.113-117.

Tseng, C., Yamaguchi, M. and Ohmori, T. (1997). Thermal conductivity of polyurethane foams from room temperature to 20 K. Cryogenics, 37(6), pp.305-312.

Fao.org. (2019). 5. Thermal insulation materials, technical characteristics and selection criteria. [online] Available at: http://www.fao.org/3/y5013e/y5013e08.htm [Accessed 2 Jan. 2019].

Engineeringtoolbox.com. (2019). Overall Heat Transfer Coefficient. [online] Available at: https://www.engineeringtoolbox.com/overall-heat-transfer-coefficient-d_434.html [Accessed 2 Jan. 2019].

Engineeringtoolbox.com. (2019). Thermal Conductivity of common Materials and Gases. [online] Available at: https://www.engineeringtoolbox.com/thermal-conductivity-d_429.html [Accessed 2 Jan. 2019].

Costa, R. (2013) ‘Strategic Map o f Industry’, pp. 1–3.

Mmf.de. (2019). Machine Monitoring. [online] Available at: https://www.mmf.de/machine_monitoring.htm [Accessed 2 Jan. 2019].

Lionprecision.com. (2019). Vibration Measurement; Vibration Sensors; Measure Vibration Precisely. [online] Available at: http://www.lionprecision.com/tech-library/appnotes/general-0020-vibration-measurement.html [Accessed 2 Jan. 2019].

S+S Regeltechnik. (2019). ATF 1. [online] Available at: https://spluss.de/en/products/temperature/temperature-passive/outside-temperature-sensor/atf-1/ [Accessed 2 Jan. 2019].

Mitsubishi-electric.co.nz. (2019). MSZ-LN25VGV Black Diamond LN25 High Wall Heat Pump with HyperCore // Mitsubishi Electric. [online] Available at: http://www.mitsubishi-electric.co.nz/heatpump/i/69301B/black-diamond-ln25-high-wall-heat-pump-with-hypercore [Accessed 2 Jan. 2019].

Solidworks.com. (2019). 3D CAD Design Software. [online] Available at: https://www.solidworks.com/ [Accessed 2 Jan. 2019].

Anon, (2019). [online] Available at: https://www.ansys.com/ [Accessed 2 Jan. 2019].

Bonsel, J., Fey, R. and Nijmeijer, H. (2004). Application of a Dynamic Vibration Absorber to a Piecewise Linear Beam System. Nonlinear Dynamics, 37(3), pp.227-243.

Dai, X., Wang, M., Zhao, Y. and Zhou, J. (2009). Self-mixing interference in fiber ring laser and its application for vibration measurement. Optics Express, 17(19), p.16543.

Deng, H. and Gong, X. (2008). Application of magnetorheological elastomer to vibration absorber. Communications in Nonlinear Science and Numerical Simulation, 13(9), pp.1938-1947.

Jacquot, R. (1978). Optimal dynamic vibration absorbers for general beam systems. Journal of Sound and Vibration, 60(4), pp.535-542.

Templeton, D. (1993). Noise and vibration control engineering: Principles and applications. Applied Acoustics, 39(3), pp.231-232.

Zeng, Y. and Forssberg, E. (1994). Monitoring grinding parameters by vibration signal measurement - a primary application. Minerals Engineering, 7(4), pp.495-501.

Liu, Y., Dong, X., Shum, P., Yuan, S., Kai, G. and Dong, X. (2006). Stable room-temperature multi-wavelength lasing realization in ordinary erbium-doped fiber loop lasers. Optics Express, 14(20), p.9293.

Zhou, X., Jeffries, J. and Hanson, R. (2005). Development of a fast temperature sensor for combustion gases using a single tunable diode laser. Applied Physics B, 81(5), pp.711-722.